INFN - Laboratori Nazionali di Frascati

Servizio Documentazione

LNF-87/23(P)

12 Giugno 1987

M. Spinetti:

STREAMER TUBES: FEATURES AND THEIR USE

Presented at the:
"Hadronic Physics at Intermediate Energy"
Proc. of the Winter School II° Course
Folgaria, February 1987

Servizio Documentazione
dei Laboratori Nazionali di Frascati
P.O. Box, 13 - 00044 Frascati (Italy)

INFN - Laboratori Nazionali di Frascati
Servizio Documentazione

LNF-87/23(P)
12 Giugno 1987

STREAMER TUBES: FEATURES AND THEIR USE

Mario SPINETTI
INFN - Laboratori Nazionali di Frascati, P.O. Box 13, 00044 Frascati (Italy)

A review on the streamer tubes developed in Frascati is presented: in particular their main features, the components and their various applications in high energy experiments.

1. INTRODUCTION

A lot of work has been invested in developing the streamer tubes technique since 1976 in Frascati, essentially by E. Iarocci and his group (Ref. 1).

The efforts were put in studying both the gas discharge regime and the cathode trasparency to streamer electric signals. The whole of these two feature has determined the success of this flexible and reliable technique.

The basic feature of the streamer regime were established by Charpak et al. (Ref. 2) and by Fisher et al. (Ref. 3) in 1977 with a systematic work following, since 1975, the preliminary studies around a gas discharge regime giving large signals (Ref. 4) . Later on a direct streamer observation was performed by Alekseev et al.(Ref. 5) and via image intesifier by Atac et al. (Ref. 6) .

The development done in Frascati on the streamer regime has determined the relevant parameters for achieving a safe and noiseless streamer regime (Ref. 7) and the suitable materials for a resistive cathode (Ref. 8). The graphite coated PVC turned out to be the most suitable material for a sufficiently high resistivity to allow the full trasparency to the fast pulses of streamer discharge.

This development has led to a first generation of streamer tubes : circular, 2 cm in diameter, 1÷2 m long and various pickup systems. In 1977 they were used in the $\gamma\gamma$-2 inner detector (Ref. 9) (≈300 tubes) at Adone and in DM2 detector (Ref. 10) (≈3000 tubes) at Orsay .

The possibility of a safe streamer regime in small tubes (≈1x1 cm^2) was exploited in 1979 for the CHARM detector implementation (Ref. 11) (≈20000 Al tubes).

The second generation of streamer tubes was conceived for the NUSEX experiment in the Mont Blanc tunnel (Ref. 12), in order to face the problem of the needed large production (≈50000 tubes).

These tubes have a 9x9 mm^2 cross section, a 3÷4 m length and are 8-folded in an open PVC profile, allowing an easy graphite coating process and a simple wiring. A graphited cover close the square cell with a symmetric electric field. The track localization is performed via an X,Y coordinates system realized with orthogonal pickup strips placed outside the streamer tubes layer and digitally readout (see Fig. 1). Several experiments were performed with this standard of streamer tubes and also many tests for the LEP future experiments.

Since 1982, after the success of the NUSEX detector, many LEP experiments decided to base hadron tracking calorimeters on the streamer tubes with a foreseen total number of streamer tubes

≈10 times bigger than the previous one with length around 8 m : so it was necessary to develop in Frascati a third generation of streamer tubes to solve the engineering problem of such a large production.

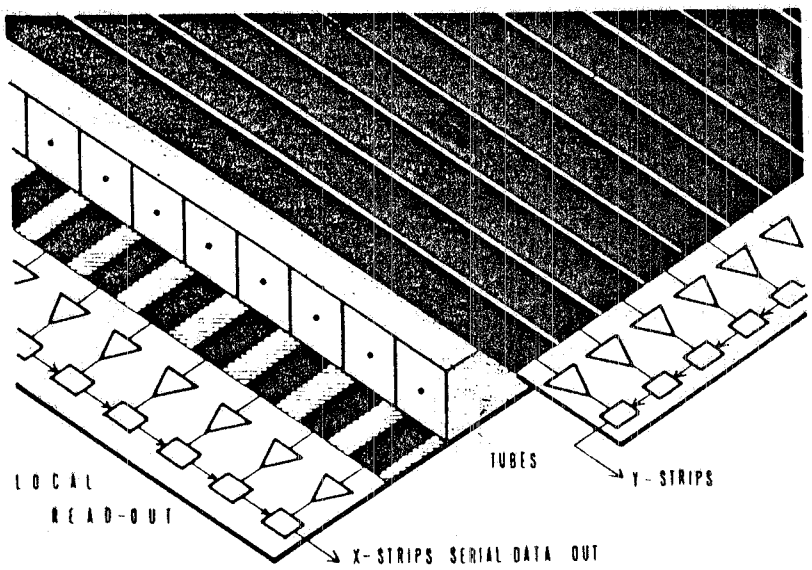

FIG. 1 - Schematic structure of streamer tubes layer in the NUSEX experiment. Tubes, X,Y strips and digital readout electronics are shown.

The basic structure of the streamer tubes was simplified, in particular adopting the coverless configuration (Ref. 13) and designing the PVC components of the streamer tubes together with the machines needed for a semi-automatic assembling procedure.

Up to now about 30 experiments are based on streamer tubes and the total number of streamer tubes already produced or on the way to be produced is approaching 10^6.

In the following I will describe the basic features and the basic components of the streamer tubes and their uses in the various experiments.

2. STREAMER TUBES COMPONENTS

The basic component (see Fig. 2) of the streamer tubes is an open comb-type 1 mm thick PVC profile delimiting 8 square cells with a 9x9 mm^2 cross section.

These profiles are coated with colloidal graphite and the resulting surface resistivity must be ≥ 100 kΩ/square in order to have a full cathode trasparency for fast electric signals.

A 100 μm beryllium-copper anode wire is streched inside each cell, kept centred by suitable spacers every 50 cm and soldered at the two ends on printed boards.

This profile is located inside a single gas-tight PVC jacket closed, at the two ends, by two PVC endcaps. Through these endcaps high voltage is supplied in parallel to the 8 wires, through a 220 Ω matching resistor for each wire.

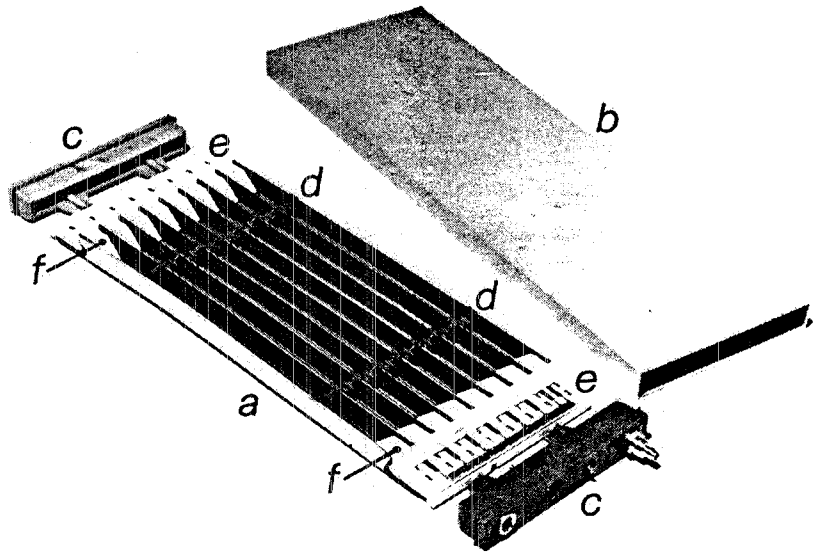

FIG. 2 - Basic components of a streamer tube : a) comb-type profile, b) gas-tight jacket, c) endcap with HV and gas connections, d) spacers, e)printed bords with 220 Ω matching resistors, f) wire.

Gas connections are on both side and the standard Ar / C_4H_{10} gas mixture (1:3) passes in parallel through the 8 tubes with a moderate flow.

The individual wires are not available through the endcaps so the streamer localization must be done via pickup electrodes facing the two available sides of a streamer tubes layer.

2.1. THE STREAMER REGIME

The streamer regime has a lot of advantages with respect to other regimes: safe and uncritical in the choice of parameters, stable and noisless and gives high and fast electrical signals.

Hereafter is a brief description of the streamer regime.

The first stage of the process is similar to the proportional regime: the primary electrons, created by the crossing particles (~100 ions pairs/cm for a minimum ionizing particle), drift towards the anode wire and as soon as the electric field becomes larger than ≈ 10 KV/cm, the electrons start to multiplicate, leaving back a wedge shaped cloud of positive ions, i.e. an avalanche (Ref. 14,15).

The standard parameters for a good operation in proportional mode are a very small diameter wire (tipically ≈20 μm) and a low value for the high voltage (HV ≈2 KV) applied to the wire . In this conditions the bulk of multiplication ($\approx 10^6$) takes place close to the wire (few μm) generating a cloud surrounding the wire. The electrons are collected on the wire but they can move only when the positive ions migrate towards the cathode. The electrical signal generation is then due to the ions migration.

For the streamer regime it is necessary to use a larger diameter for the wire (tipically ≈ 100 μm) and a higher HV value (≈4.5 KV) : so the region, where the electric field is larger than ≈10

KV/cm, is wider and extends up to ≈1 mm from the wire. So the moltiplication takes place in the same way of the proportional mode but farer away from the wire so that, during the avalanche advancing towards the anode, the number of e^- in the front edge of the avalanche can exceed $\approx 10^8$.

Now the dipolar field, created by this space charge, is so high inside the avalanche pratically to negate the applied field. As a consequence, the recombination takes place inside the avalanche and hard photons (≈11eV) are emitted isotropically, generating other ions pairs within a range of few hundred microns (limited by the quenching gas concentration).

These secondary electrons can generate new avalanches only if they are behind or in front of the primary avalanche, where the applied electric field is reinforced by the space charge dipolar field. These new avalanches merge to the previous contributing to form a space charge filament, i.e. the streamer, advancing towards the cathode and the anode with a speed of $\approx 10^8$ cm/s (Ref. 16).

This filament has a diameter of ≈200 μm, a length of 1÷3 mm and is oriented from the wire side towards the arrival direction of the primary electrons. The formation time is tipically few nanoseconds corresponding to the risetime of the electric signal.

The quenching of the cathode streamer tip is due to the combined action of the quenching gas whose high concentration limits the range of hard photons and the electric field shaped as 1/r which at distances bigger than ≈1mm does not favorite the growing of secondary avalanches even if the electric field on the tip is reinforced by the space charge.

In Fig. 3 beautiful photographs of individual streamers, taken by Atac et al. (Ref. 6), are reported.

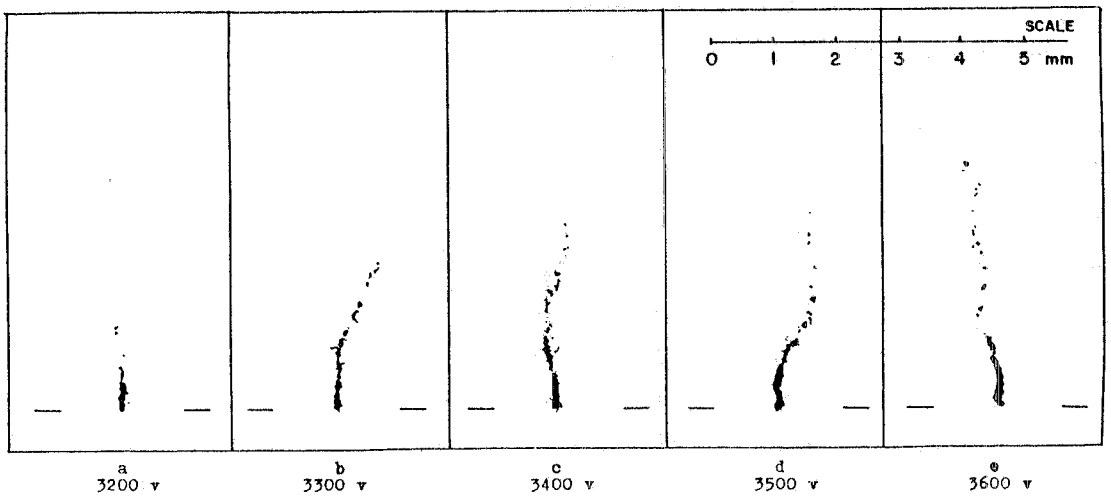

FIG. 3 - Individual streamer at various voltages.Anode wire is indicated.

Being the space charge distributed far from the wire, the electric signal is due to the electrons collection: the fast rise time (few ns) corresponds to the formation of the streamer while the long tail (≈50 ns) is due to the slow arrival of the electrons on the anode wire.

In Fig. 4 (Ref. 6) the collected charge as function of applied HV is shown: the transition

between the proportional and streamer mode appens as soon as the limit of $\approx 10^8 e^-$ is reached in the primary avalanche giving place to the recombination phenomena. This large discontinuity in amplification explains the noiseless electrical signal and the large efficiency plateau.

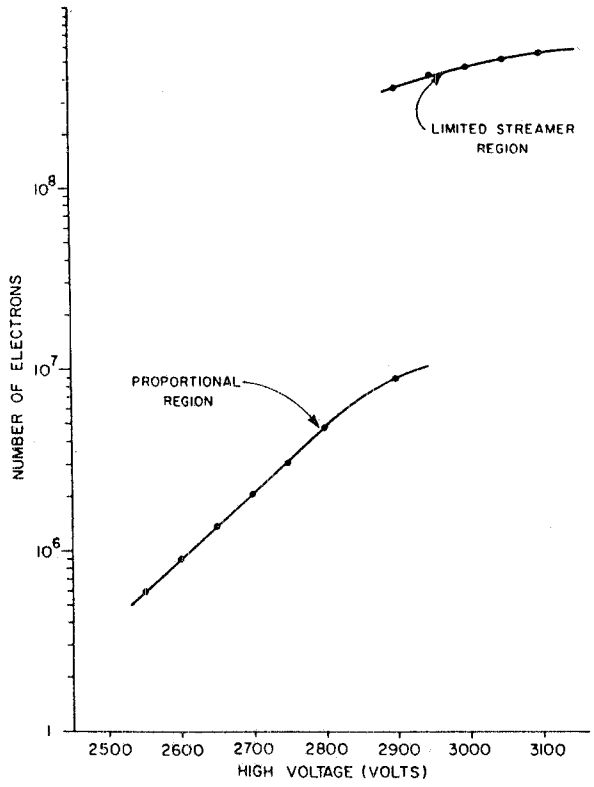

FIG. 4 - Measured charge as a function of the high voltage.

In Fig. 5 a typical single rate curve is shown (Ref. 13). The low voltage rise corrisponds to a gradual transition from proportional to streamer regime and the high voltage rise corresponds to spurious streamers generated by either gas and surfaces impurities or ions feedback.

The streamer charge in the standard work condition (100 V over the plateau knee, gas mixture Ar / Isobutane (1:3)) is about 30 pc ; the charge variation with the HV value typically is ≈20% for 100 V change inside the plateau . The pulse shape does not change when the HV varies inside the plateau, while the pulse peak can change a factor ≈4 for a variation of 700 V inside the plateau (Ref. 1,6,17).

The streamer charge distribution (Fig. 6) typically has a small long tail due to δ-rays, but is rather narrow around the peak value (σ=25÷30%) for normal incidence particles : this is indicative that the streamer regime is a saturated one. Nevertheless there are measurements (see below) which indicate the streamer charge to be affected by large amount of initial ionization: a possible interpretation is that the higher the initial ionization, the earlier the $\approx 10^8 e^-$ are reached, the bigger the streamer can be.

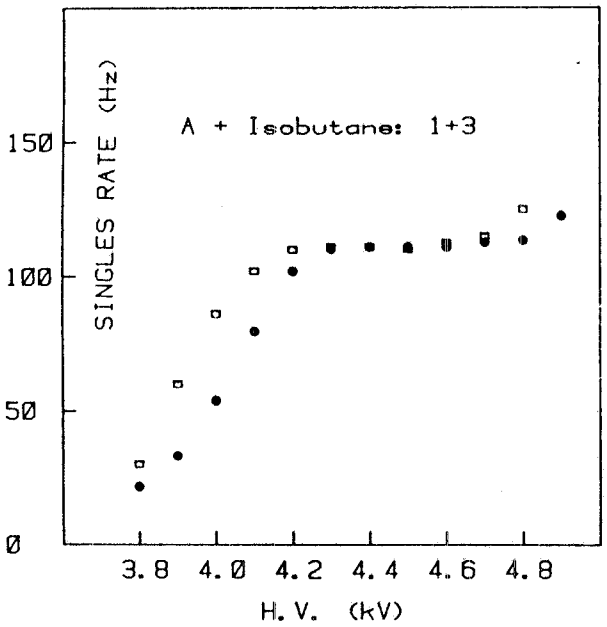

FIG. 5 - Single conting rate plateau for standard tubes (square) and coverless tubes (dots).

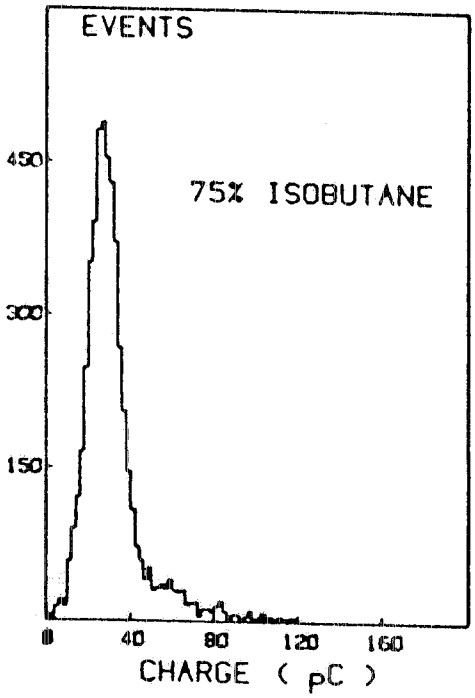

FIG. 6 - Streamer charge distribution in standard condition for normal crossing particles.

2.2. GAS MIXTURE

The most important component for the streamer regime is the gas mixture: its quenching action is essential to have an uncritical and noiseless streamer regime.

The basic elements of the mixture are essentially the same used in the proportional regime, being similar the elementary processes in gases, but a higher quenching action is needed due to the more abundant hard photons production.

In the commonly used gas mixture the basic element is a noble gas because these gases, with respect to polyatomic gases, have an higher multiplication factor at lower electric field. Between noble gases argon is one of the best, having an high number of ion pairs released by minimum ionizing particles and being very cheap.

In pure argon the multiplication process cannot be controlled and easely degenerate in a continuos discharge. So a second type of gas is needed, that is a polyatomic gas like hydrocarbons or CO_2. These gases, being rich of non radiative rotational and vibrational levels, have an high efficiency in many roles: to degrade the argon recombination photons (≈11 eV), to quench the discharge propagation mechanism, to neutralize by charge-exchange the argon ions during the path towards the cathode (this avoides the hard photons emission when argon ions neutralize on the cathode) , to reduce the gas thermal energy growth under the electric field action (this allows the "saturated" e^- drift velocity, ≈5 cm/μsec) .

The type and the concentration of the hydrocarbon is then dictated by the needed quenching power in the various configurations.

In the streamer regime the criteria in determining the minimum quencher concentration is that the streamer must be limited enough to leave a sufficient space between the streamer tip and the cathode surface in order to avoid secondary electrons extraction from cathode, which could generate secondary straemers (afterpulses). So the smaller the tube diameter, the higher the needed quenching power is.

In practice, for small tubes (diameters $\leq \approx 1$ cm) the most efficient and suitable quenching gas is the Isobutane (C_4H_{10}), which moreover does not present any long term degeneracy effect. Its useful concentration is in the range ≈50÷90%, according with the tube diameter.

For bigger tubes also less efficient quencher can be used with a proper concentration (ethane, propane, etc.).

With respect to the electric signal, it has to be notice that, reducing the quencher concentration, the pulse tail becames longer (Fig.7) (Ref. 17): a propable interpretation is that the streamer becames fatter due to the side avalanches whose collection time is longer for the reduced electric field. As a consequence the streamer charge depends rapidly on the quencher concentration (Fig.8).

It is relevant to note that, despite the loose in electric signal, the higher the quencher contration is, the larger the efficiency plateau is, due to a lower sensitivity to spurious effects.

In case, for safety reason , the use of high percentage of isobutane is to avoid other mixture can be used: for example in the Nusex experiment (Ref. 12) the mixture Ar / CO_2 / n-pentane (1:2:1) has been used, replacing the standard Ar / Isobutane (1:3) without any major difference.

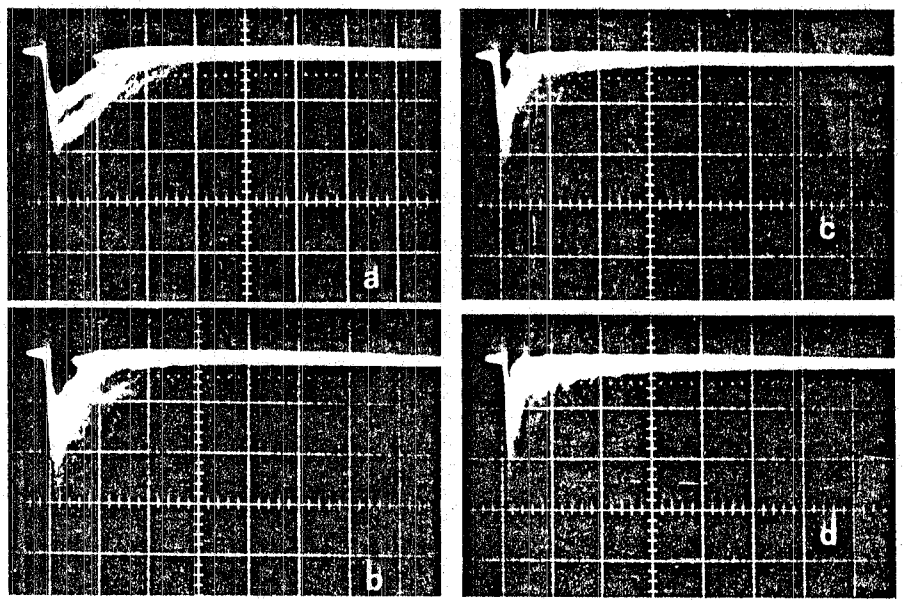

FIG. 7 - Wire pulses for different isobutane fraction: a) 50%, 2.8 kV, b) 60%, 3.1 kV, c) 70%, 3.3 kV, d) 80%, 3.7 kV.

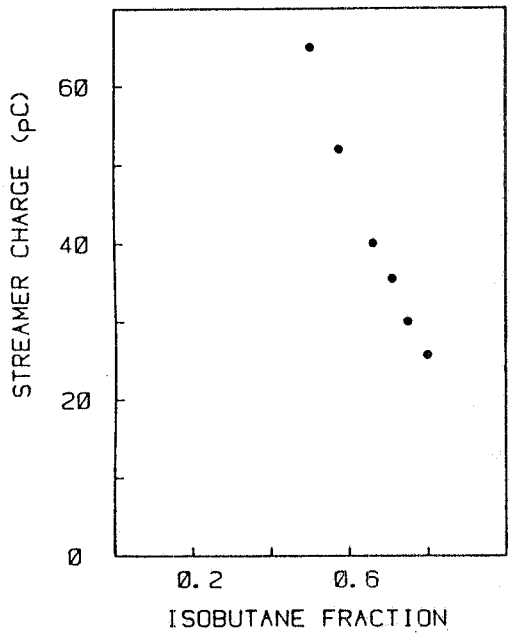

FIG. 8 - Single streamer peak charge vs. isobutane fraction.

2.3. CATHODE MATERIALS

The cathode material does not affect the streamer process but have a clear influence on the working parameters of the tubes. As above mentioned, when the streamer tip is too near to the cathode , the photons emitted by the streamers can extract secondary elctrons which, after a time corrispondent to the drift time between cathode and wire (≈150 ns), can generate others streamers in an iterative process. In case of a material with lower electron work function it has expected a worst sensitivity to this mechanism. This can be recovered by the use of a bigger quenching action

A comparison between the standard cathode material (the PVC coated with graphite) and Al has confirmed this mechanism (Ref. 17) : for the same gas mixture, the single rate plateau, performed with two different dead time (200 ns and 1000 ns) shows that in the Al case a 10% afterpulses contribution start 500 V earlier with respect of the PVC case (200V above the knee with respect 700V).

2.4. CATHODE TRASPARENCY

The cathode trasparency is the second component which has determined the success of this technique. The cathode trasparency gives the possibility practically to separate the gas discharge process from the pickup system, allowing the maximum freedom in designing the coordinate system and permitting moreover twice the use of the same tubes layer.

The standard material for a trasparent cathode is a good isolant (like PVC) coated with a resistive varnish done with colloidal carbon. The thickness of the varnish layer determines the resistivity of the cathode which is measured in Ω/square .

Intuitively the cathode trasparency works in a very simple way: a space charge, created inside the tube, i.e. the streamer, induces on the surrounding electrodes an equivalent charge. If the

cathode resistivity is above a certain threshold, the charges mouve slowly on the cathode so that the shielding action of the cathode cannot take place and induced pulses are seen on the electrodes placed outside the tube cathode.

However the cathode resistivity cannot be much too high, otherwise the charged ions accumulate on the cathode and severe limits in counting rate could arise. The relevant fact is that a large plateau can be found, where the streamer tubes can safely work (roughly from ≈100KΩ/square up to ≈10 MΩ/square) .

Analyzing in more detail the cathode trasparency, the most relevant parameter is the time costant T_c=RC (R=cathode resistivity, C= capacitance of the actual pickup strips and tubes geometry) compared with the streamer pulse length T_s . The trasparency plateau begins when $T_c \gg T_s$. It has to be notice that, in case of analog readout, the relevant time is not T_s but the integration time (Ref. 18).

An exact computation of the trasparency plateau is not reliable, being necessary to take in account in detail all the distributed parameters of the actual geometry (dielectric thickness, tubes wall, strips length, etc.). The most simple way is to test it using, as a sensible parameter, the ratio R between the pulse on the central strips (faced to the streamer) and the adiacent strips. As shown in Fig.9 (Ref. 18), when R is well inside the trasparency plateau (R≈6) the pulses induced on the two strips reproduce the wire signal (negative sign) and no distorsion appears, being slow the charges movement on the cathode.

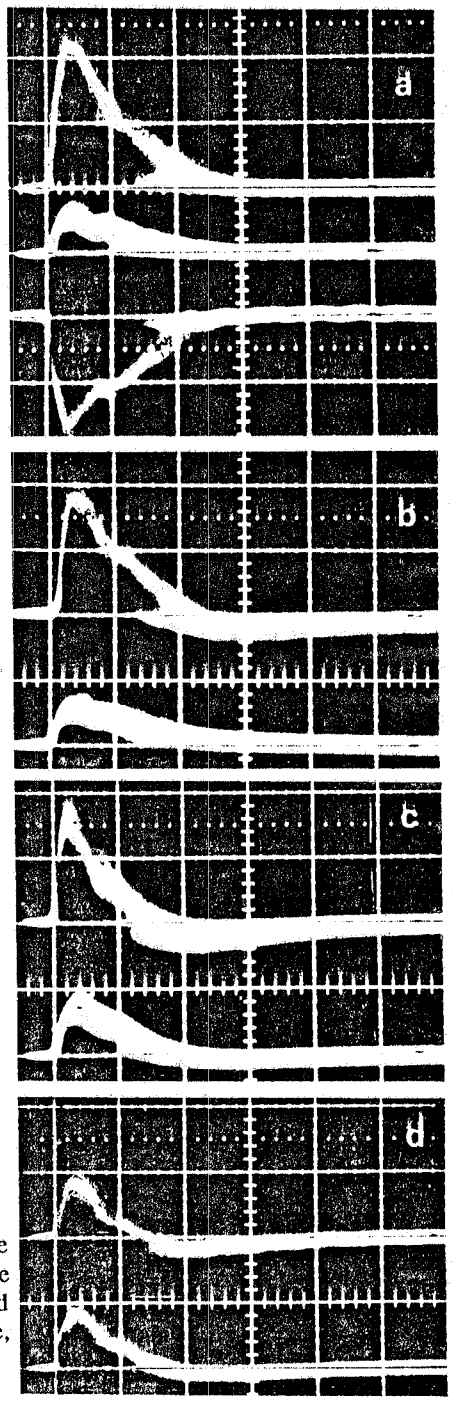

FIG. 9 - a) Pulses (terminated on 50 Ω) on the central strip, side strip and wire, for cathode resistivity 7 MΩ/square. Pulses on central and side strips for: b) 200 kΩ/square, c) 30 kΩ/square, d) 10 kΩ/square.

When R becames lower and lower (R≈1), outside the trasparency plateau, more and more charges mouve faster towards the area facing the the streamer, reducing the pulse on the central strip, reinforcing the pulses on the adiacent strips and differentiating the induced pulses. So, in case of digital readout, a lower resistivity can have a moderate effect in reducing the spatial accuracy and

the efficiency; on the contrary, in case of analog readout, the effect can be important because, in the integration time, the negative pulse tail gives a subtractive contribution which can reduce the integrated charge still down to zero.

2.5. PICKUP ELECTRODES

The pickup electrodes, outside the trasparent cathode, can be drawn in any way one need. The streamer signals are high and consequently also the induced signals, although reduced of a factor 1/5÷1/10, are still sufficently high to drive low impedence electrodes.

The various experiments have drawn its own electrodes to fit particular needs. The DM2 experiment used a spiral delay line wound on each couple of tubes eliminating the ambiguities in the spatial reconstraction of the tracks.

A polar (r,ϕ) coordinate system has been proposed for a UA2 upgrading to select a p_t trigger. Hadron calorimeters use rectangular pads for analog readout usually wired in towers, combined with digital strips for a projected view.

The MACRO experiment uses a diagonal coordinate to solve access problems.

However the most diffused system of coordinates is the X,Y cartesian coordinates, as that of the NUSEX experiment, with digital readout. This system is done with two strips layers, one parallel (X strips) and one orthogonal to the tubes wires (Y strips), each placed on each side of a streamer tubes layer. Each strips layer is realized with a 1 mm PVC sheet with glued on the two sides a ground 40μm Al sheet and the 40μm Al strips: Y strips are 1.2 cm pitch and 1 cm wide, while X strips are 1 cm pitch (equal to the tube pitch) and only 0.4 cm wide in order to reduce the crosstalk. The strips have an impedence approximatly 50Ω, a propagation time ≈6 ns/m and a very long attenution length (≈20 m).

Concerning the induced pulses, the X strips show a rather complex behaviour with respect to the Y strips. For Y strips the streamer injects a current in the point of the strip-ground line where the streamer is generated; for X strips the streamer injects the current in the wire-strip line. This current, at the HV connections, is than injected in the strip-ground line as for Y strip. Due to this fact, the total induced charge has a maximum spread in time of $2t_s$ (t_s being the strip propagation time) when collected at the opposite side with respect to the HV side, while it is $4t_s$ when the charge is collected at the HV side. For long tubes, this effect gives a preference for placing the readout electronics on the side opposite to the HV side (Ref. 8).

Concerning the digital readout, there is one low threshold discriminator (≈2 mV, adjustable) for each strip. At the event time, the status of these discriminators is memorized in a shift register as long as the total number of strips to be read. The shift register configuration is then serially read by a computer.

3. USE OF STREAMER TUBES

The most natural use of this technique is in sampling calorimeters.

The reliability and simplicity in running this detector, the intrinsec good granularity, the easy and

cheap construction technology favorite the use of a large amount of streamer tubes as required for large tracking calorimeters, where not only the shower energy is needed but also the event pattern to recognize the topology and to measure the spatial localization.

Moreover in the various applications of this technique, also other aspects have being exploited either optimizing the calorimeter parameters or developing special techniques.

In the following I will describe some of the most typical use of streamer tubes, which, on the other hand, are often mixed together in the experiments.

3.1. TRACKS DETECTORS

The intrinsic spatial accuracy of streamers tubes with digital readout of strips or wires is essentially related to the tube diameter: for 1 cm^2 tubes with the standard X and Y strips, the spatial resolution is $\sigma_x \approx 3$ mm and $\sigma_y \approx 4$ mm (Ref. 12).

This natural accuracy can be increased using more sophisticated electronic systems, different for the two views.

The longitudinal view can be implemented with the readout of the electrons drift time (delay between the wire signal and an external trigger). Preliminary tests give a spatial resolution $\sigma_x \approx 500$ μm which propably can be ameliorate via software corrections.

In the transverse view, using the charge centroid with the analog readout on the Y strips, the UA1 experiment has obtained a spatial resolution ≈ 600 μm .

3.2. PARTICLE DISCRIMINATION

Particles like π , μ , $e^{\pm}$ have a very different way of interacting with the matter. In streamer tubes calorimeters with digital readout, the good granularity allows to study in details the pattern of deposited energy so that a good discrimination between these particles cathegories can be achieved. Moreover calorimeters hardware parameters can be optimized in order to achieve a better discrimination.

a) π / $e^{\pm}$ discrimination

A difficult aim is to recognize low energy electrons (≤~1GeV) in a high π background. Two experiments, APPLE at LEAR (Ref.19) and R422 at ISR (Ref.20), have used two calorimeters specially designed to this aim. In particular, the depth of the calorimeter was limited to only ≈7 r.l. to reduce the number of showering π, without efficiency losses for electrons. Moreover the sampling pitch was enlarged in order to increase the lateral e.m. shower spread and to maximize the differences with π. The readout was based on X,Y strips with digital electronics: a low thresholds set favorites an higher shower multiplicity. With a simple hits counting and with other software criteria based on the digital pattern, a π/e discrimination better than 10^{-3} was achieved in the energy range 0.5÷4 GeV (Fig. 10, Ref. 20).

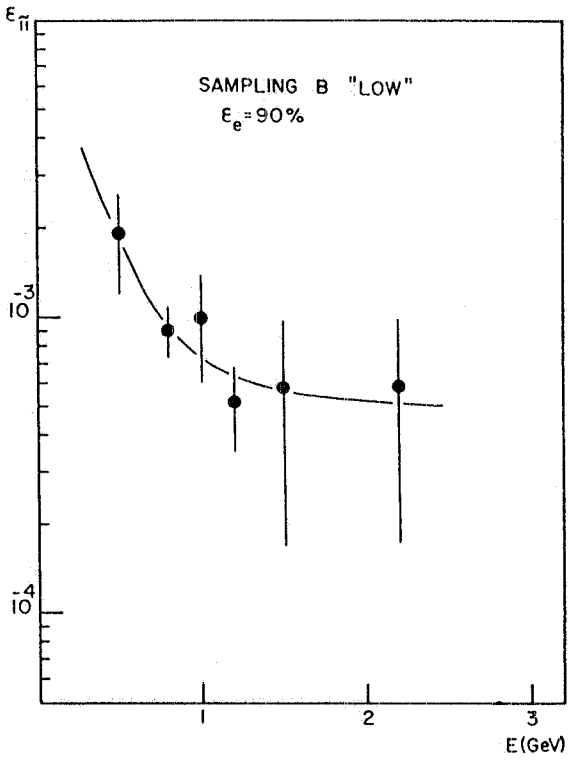

FIG. 10 - Pion rejection factor vs. beam energy for $e^{\pm}$ detection efficiency of 90%.

b) π / μ discrimination

Another interesting application is the μ identification, i.e. a straight track, inside hadronic showers, performed with the test calorimeter of the ALEPH experiment (Ref. 21).

The calorimeter has a combined digital and analog readout (see after).Taking into account several software criteria based on the digital pattern and the energy deposition of the shower, a likelihood method has been developed. This method allows to correctly classify, in the ≥99% of cases, π events, μ events and overlapped $\pi+\mu$ events.

3.3. DIGITAL CALORIMETERS

The aims of these calorimeters, or tracking calorimeters, is to give at the same time the topology, the spatial localization and the energy deposition of the events.

The basic structure is an alternated sandwich of absorber layers (usually Fe or Pb) and streamer tubes layers (1x1 cm^2 cell). The pickup system is typically done with orthogonal X,Y strips with a digital readout . The electronic threshold on each strip is typically few mV and determines the mean number of fired strips; when a clear pattern is needed the threshold must be as high as possible without efficiency losses and the mean strips multiplicity turns out to be n_x = 1.1 and n_y =1.6 for m.i.p. with normal incidence. The absorber thickness and packing density of the layers are choosen in order to match the experimental needs. At energies around ≈1 GeV, they can give a powerfull pattern of the event with high granularity : as an example, topology of tracks and showers plays a very important role in recognizing a proton decay event or an anti-n annhilation star.

The first large scale experiment is the NUSEX experiment (Ref.12), for which this technique has been developed : than other experiments have used the same technique, as the two experiment searching n—anti-n oscillations at the Grenoble reactor (the second one is under construction) or the FENICE experiment (Ref. 22) (n—anti-n form factor) for ADONE e^+e^- storage ring, now under construction, or the ANTIN experiment (Ref.23) (p—anti-p and n—anti-n esperiment at LEAR).

The energy response for showering particles is not the best one can achieve with streamer tubes calorimeters: the shower energy is simply calculated via the total number of hits which, at low energy (below ≈ 1 GeV), is a sampling of the shower total track length. This method, at higher energies, undergoes rapidly to a lose in linearity when the track density is high enough and the double occupancy of the same sensible cell (1 cm^2) becomes not negligible. The energy resolution, in the linear region, scales as $\sqrt{E}$ and is comparable with the achievable resolution when using scintillation counters.

3.4. ANALOG CALORIMETERS

In order to push at higher energies the linear energy response of streamer tubes calorimeters, the analog readout of the streamer charge has been implemented.

In this case the streamer itself can be roughly thought as a 10 times smaller sensible cell (≈ 1 mm of wire). So the total charge is still proportional to the shower total track length.

With respect to other proportional regimes, the advantage of using the streamer saturated regime is also that the long Landau tail, due to long δ-rays passing along a tube element, give in any case a limited contribution as if the steamer could saturate ≈ 3 mm of wire.

Using both sides of a streamer tubes layer, the charge readout can be combined with a digital readout so that, at the same time, a good energy measure and a high spatial accuracy is available.

This kind of calorimeters for e.m. showers are not frequent in experiment: other techniques, although more difficult and more expensive, are present with higher resolution and compactness. Nevertheless the performances of test calorimeters (Ref. 24) are interesting : linearity is good up to ≈20 GeV and the energy resolution is $.13\sqrt{E}$ slowly increasing with energy indicating that losses in the shower core and δ-rays play a role still in the linear region.

On the contrary the last few years have seen a large application of this technique for hadron calorimeters. Three big experiments at LEP, ALEPH, DELPHI and OPAL, and the SLD experiment at SLAC Linear Collider are mounting ≈320000 streamer tubes of the standard type developed in Frascati. These calorimeters use the iron yoke of the magnetic field, segmented in 5 cm slabs and instrumented with streamer tubes layers : the readout is analog for trapezoidal pads wired in towers and digital (longitudinal strips) in the view parallel to the beams. This combination permits both a good spatial resolution and an energy resolution comparable with more sophisticated techniques and a powerfull pattern in the longitudinal view, which in e^+e^- experiments is the most interesting. The depth of these calorimeters is typically ≈ 6 interaction length. Several tests on prototype calorimeters have been done and the results indicate a linear response up to 50÷100 GeV

and an energy resolution about $0.8\sqrt{E}$ (Fig.11, Ref. 25), which is tipycal when iron is used as absorber. Infact a test, done with copper absorber, shows a better resolution of $\approx 0.6\sqrt{E}$, as expected (Ref. 26).

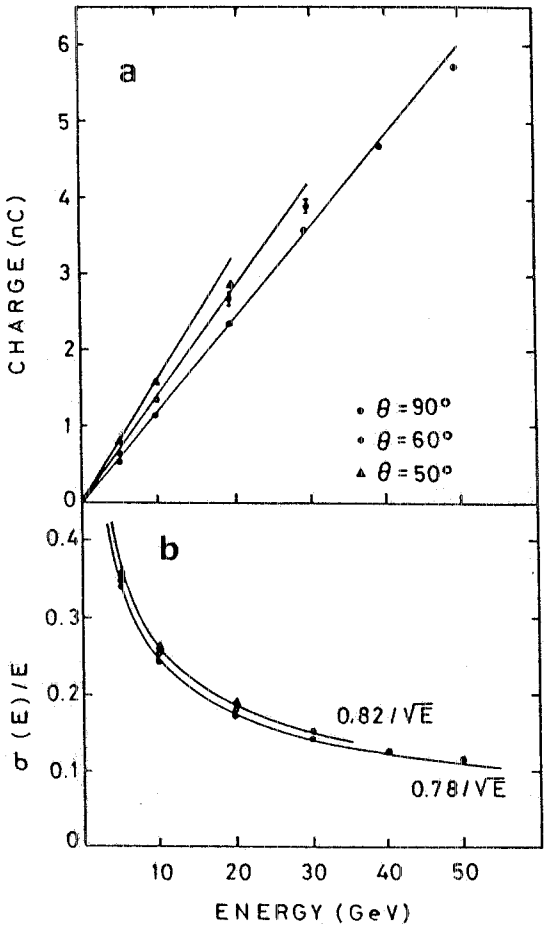

FIG. 11 - Charge response (a) and energy resolution (b) for pions in standard conditions.

3.5. THE MACRO EXPERIMENT

A remarkable evolution of streamer tubes is rappresented by the new standard developed for matching the special needs of an underground experiment.

MACRO is a large area detector to be installed in the GRAN SASSO Underground Laboratory for searching monopoles, other rare massive particles and for studying cosmic rays. The special needs of the experiment can be summarize in the following points:

-the coverage of large area $\approx$ 15000 m^2 of streamer tubes);

-the highest reliability, being the experiment underground and in continuous run for many years;

-low threshold for ionizing particles in order to extend at very low β the monopoles sensibility;

-a rough measure of the particle dE/dx as a check for very high ionizing particles.

The new version can be as long as 12 m, has a 3x3 cm^2 coverless tube cross section and a cathode resistivity $\approx$500 Ω / square. Besides the reduction of the total streamer tubes number, these peculiarities increase the already good reliability of the 1x1cm^2 streamer tubes, as can be deduced from the $\approx$1000 V large singles counting rate plateau (Ref 27).

At $\approx$ 500 V inside the singles plateau, a full efficiency for a single ion pair is achieved, giving the lowest possible threshold for ionizing particles (Ref 28).

Now, the tubes have only one trasparent side, the coverless side, which is utilized for the diagonal strips; the X view is determined by reading the wire signals.

Although the streamer regime is a saturated one, the streamer charge grows when the ionization realesed by the crossing particle increases. Tests have been done using relativistic heavy ions with different Z. The result is a linear increase with log Z of the streamer charge distribution peak (Ref. 27). As already mentioned, the peak of the streamer charge distribution is a measure of the streamer charge disregarding of the δ-rays production. Infact δ-rays are responsible onlt for the long tail in the streamer charge distribution. The monopole, being very slow, have not such a contribution so this calibration gives the possibility to check the high ionizing power of the monopole (Fig. 12, Ref. 27).

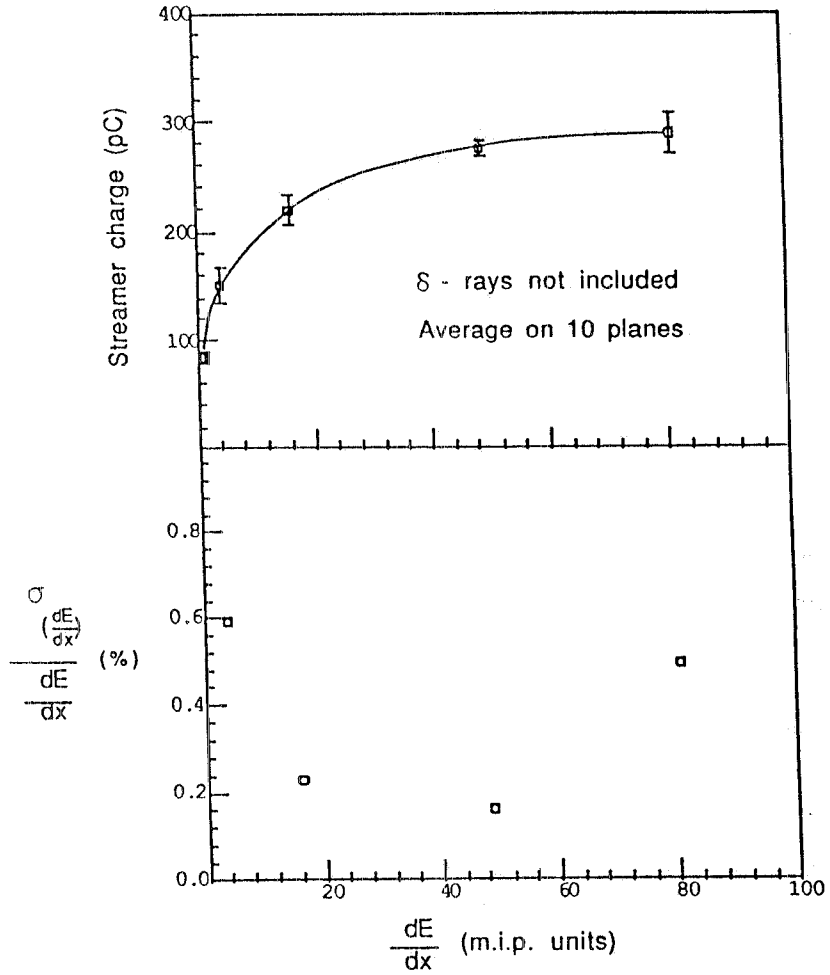

FIG. 12 - Streamer charge peak and resolution vs. dE/dx (in terms of m.i.p.), averaged over 10 streamer tubes planes.

4. CONCLUSIONS

The streamer tubes technique is now a succesful one in many application and in particular in large traking calorimeters. The constraction simplicity, the reliable operation , the flexibility for the readout systems, the noiseless regime have played an essential role in determining this success, even when the performances were not the best one can achieve.

The last standard, the MACRO standard is so simple and reliable that can now be produced by external firm. Other development are under study in order to increase, if possible, the constraction simplicity and the reliability for smaller diameter tubes. At this level , this technique is ready for very large future experiments.

REFERENCES

1) For a review paper see:
E. Iarocci, Nucl. Instr. and Meth. 217(1983)30
2) G. Charpak et al., IEEE Trans. Nucl. Sci. NS-25(1978)122
3) J. Fischer, Nucl. Instr. and Meth. 151(1978)451
4) S. Brehil et al., Nucl. Instr. and Meth. 123(1975)225
5) G.D. Alekseev et al., Lett. Nuovo Cim. 25(1979)157
6) M. Atac et al., Nucl. Instr. and Meth. 200(1982)345
7) G. Battistoni et al., Nucl. Instr. and Meth. 164(1979)57
8) G. Battistoni et al., Nucl. Instr. and Meth. 176(1980)297
9) C. Bacci et al., Phys. Lett. 86B(1979)234
10) J.E. Augustin et al., Phis. Scripta 23(1981)623
11) M. Jonker et al., Nucl. Instr. and Meth. 215(1983)361
12) G. Battistoni et al., Nucl. Instr. and Meth. A245(1986)277
13) G. Battistoni et al., Nucl. Instr. and Meth. 217(1983)429
14) F. Sauli, CERN 77-09 (1977)
15) G. Charpak et al., Nucl. Instr. and Meth. 162(1979)405
16) P. Rice-Evans, Spark, streamer and prop. chambers, Richelieu Press
17) G. Battistoni et al., Nucl. Instr. and Meth. 217(1983)433
18) G. Battistoni et al., Nucl. Instr. and Meth. 202(1982)459
19) G. Bardin et al., CERN EP 87/26
20) M. Basile et al., Nucl. Instr. and Meth. A235(1985)74
21) R. Baldini et al., Nucl. Instr. and Meth. A251(1986)449
22) R. Baldini et al., L.N.F., Internal note (to be published)
23) T. Bressani et al., IEEE Trans. Nucl. Sci. NS-32(1985)733
24) G. Battistoni et al., Proc. Workshop on Gas Sampling Calorimetry, Fermilab (1982)
25) M. Catanesi et al., Nucl. Instr. and Meth. A247(1986)438
26) B. Bleichert et al., Nucl. Instr. and Meth. A241(1985)43
27) M. Calicchio et al., Proc. Cosmic Ray Conference HE 7.2-22 Moscow (1987)
28) M. Battistoni et al., Nucl. Instr. and Meth. A235(1985)91